

The involvement of HDAC3-mediated inhibition of microRNA cluster 17-92 in hyperoxia-mediated impairment of lung development in neonatal rats

Running title: Role of HDAC3 in BPD development

Di Wang¹, **Hui Hong**², **Xiao-Xia Li**², **Jing Li**², **Zhi-Qun Zhang**^{2,*}

¹ Department of Pediatrics, Affiliated Hangzhou First People's Hospital, Zhejiang University School of Medicine, Hangzhou 310006, P. R. China

² Department of Neonatology, Affiliated Hangzhou First People's Hospital, Zhejiang University School of Medicine, Hangzhou 310006, P. R. China

* **Correspondence to: Zhi-Qun Zhang**, Department of Neonatology, Affiliated Hangzhou First People's Hospital, Zhejiang University School of Medicine, No. 261, Huansha Road, Hangzhou 310006, Zhejiang Province, P. R. China

E-mail: zhiqun.zhang@163.com

Tel.: +86-13989453622

Abstract

1
2 **Background:** The incidence of bronchopulmonary dysplasia (BPD), a chronic lung disease of
3
4 newborns, has been paradoxically rising despite medical advances. Histone deacetylase 3 (HDAC3)
5
6 has been reported to be a crucial regulator in alveologenesis. Hence, this study aims to investigate
7
8 the mechanism of HDAC3 in the pulmonary angiogenesis and alveolarization of BPD.
9

10
11 **Methods:** A hyperoxia-induced mouse model of BPD was constructed. The mean liner intercept
12
13 (MLI) and alveolar volume were measured to evaluate the alveolarization in BPD mice.
14
15 Immunofluorescence assay was performed to detect the microvessel density (MVD) of lung tissues.
16
17 Next, the expression of HDAC3 and its enrichment in the promoter region of microRNA
18
19 (miR)-17-92 cluster, as well as the enrichment of p65 in the placental growth factor (Pgf) promoter
20
21 region were detected by Western blot analysis and chromatin immunoprecipitation (ChIP) assay.
22
23 The effect of HDAC3 and p65 on the activity of miR-17-92 promoter and Pgf promoter were
24
25 examined by dual-luciferase reporter gene assay, respectively. Finally, the role of HDAC3 in
26
27 angiogenesis and alveolarization through miR-17 regulated EZH1-p65-Pgf axis was validated in
28
29 BPD mouse models.
30
31
32
33
34

35
36 **Results:** HDAC3 was involved in the regulation of alveolarization and angiogenesis in BPD.
37
38 Results demonstrated that the expression of the miR-17-92 cluster in BPD was regulated by
39
40 HDAC3. miR-17 was related to the regulatory role of HDAC3 in regulating EZH1 expression and
41
42 in lung fibroblasts of BPD. Besides, results showed that EZH1 could promote Pgf expression by
43
44 recruiting p65 to regulate BPD. HDAC3 regulated the expression of EZH1 through miR-17 to
45
46 promote the recruitment of p65 in the Pgf promoter region, thus enhancing the transcription and
47
48 expression of Pgf. HDAC3 was demonstrated to regulate Pgf through the miR-17-EZH1-p65 axis to
49
50 mediate angiogenesis and alveolarization of BPD mice.
51
52
53

54
55 **Conclusion:** Altogether, the present study revealed that HDAC3 could regulate the EZH1-p65-Pgf
56
57 axis through miR-17 in the miR-17-92 cluster in the pulmonary angiogenesis and alveolarization of
58
59 BPD mice.
60

Keywords: Histone deacetylase 3; microRNA-17-92 cluster; Placental growth factor; Bronchopulmonary dysplasia; Pulmonary angiogenesis; Alveolarization

1
2
3
4
5
6
7
8
9
10
11
12
13
14
15
16
17
18
19
20
21
22
23
24
25
26
27
28
29
30
31
32
33
34
35
36
37
38
39
40
41
42
43
44
45
46
47
48
49
50
51
52
53
54
55
56
57
58
59
60
61
62
63
64
65

Background

1
2 Bronchopulmonary dysplasia (BPD) is a common chronic lung disease characterized by arrested
3
4 alveolar development or loss of alveoli which commonly occurred in premature infants. BPD was
5
6 associated with increased risks of morbidity and mortality, as well as neurodevelopmental outcomes
7
8 among prematurely born infants [1, 2]. Risk factors responsible for BPD include pre- and postnatal
9
10 infections, hyperoxia, as well as mechanical ventilation, which not only influence the interacted
11
12 function of pro- and anti-inflammatory proteins, but also the extra alterations of signaling pathways
13
14 which is closely related to the imbalance of growth factor [3]. Although extensive approaches have
15
16 alleviated the survival of preterm infants in neonatal care, the effectiveness of the currently
17
18 available therapeutic strategies in reducing the incidence and severity of BPD remains very limited
19
20 [4]. Therefore, it is important to determine the specific molecular mechanism of BPD in order to
21
22 identify potential novel biomarkers relevant to BPD.
23
24
25
26
27

28
29 Histone deacetylases (HDACs) are chromatin-modifying enzymes that have emerged as the
30
31 important targets for treating various diseases due to their powerful regulatory role in physiological
32
33 and pathological settings [5]. HDAC3, a member of the HDAC superfamily, has been reported to be
34
35 highly expressed in adenocarcinoma of the lung and closely associated with the poor prognosis of
36
37 this disease [6]. Additionally, HDAC3 has been shown to play a pivotal role in cellular proliferation,
38
39 apoptosis as well as transcriptional repression, and may serve as a negative regulator of
40
41 angiogenesis [7]. However, the regulatory function of HDAC3 in BPD remains unknown. Evidence
42
43 has shown that the knockdown of HDAC3 could upregulate the expression of microRNA
44
45 (miR)-15a/16-1, thereby suppressing lung cancer cell growth and colony formation [8]. miRNAs
46
47 are a class of small noncoding RNAs that regulate gene expression at the post-transcriptional level,
48
49 leading to mRNA degradation or inhibition of protein translation [9]. The miR-17-92 cluster
50
51 (miR-17, miR-18a, miR-19a, miR-19b, miR-20a, and miR-92) has been reported to be poorly
52
53 expressed in lung tissues of BPD infants, while the downregulation of miR-17-92 cluster was
54
55 closely related to the development of BPD [10]. It has been shown that miR-17 could regulate the
56
57
58
59
60
61
62
63
64
65

1 expression of EZH1 which involved in the mediation of drug resistance in non-small cell lung
2 cancer, Besides, the binding of EZH1 to the p65 transcription factor could promote the transcription
3 of downstream target genes [11]. It has also been reported that p65 could directly bind to the
4 promoter region of placental growth factor (Pgf)/Plgf and transcriptionally activates the expression
5 of Pgf/Plgf [12]. Pgf has been found to be involved in the regulation of BPD, as well as acute and
6 chronic lung injury in newborn infants [13]. Therefore, it was hypothesized that EZH1 could
7 promote p65-activated transcription of Pgf in BPD mice. In the present work, we planned to explore
8 the potential effects of HDAC3 regulating miR-17 in the miR-17-92 cluster on the angiogenesis and
9 alveolarization of BPD *via* EZH1-p65-Pgf axis, which could serve as a potential target to treat BPD.
10
11
12
13
14
15
16
17
18
19
20
21

22 **Materials and methods**

23 **Ethics statement**

24
25 All animal experiments were conducted in strict accordance with the Guide to the Management and
26 Use of Laboratory Animals issued by the National Institutes of Health. The protocol of animal
27 experiments was approved by the Institutional Animal Care and Use Committee of Affiliated
28 Hangzhou First People's Hospital, Zhejiang University School of Medicine.
29
30
31
32
33
34
35
36
37
38
39

40 **Hyperoxia-induced BPD mouse model establishment**

41
42 Thirty C57Bl/6J newborn mice with an average weight of $1.36 \text{ g} \pm 0.09\text{g}$ were randomly divided
43 into one litter (equal numbers of mice per litter). The mice following BPD modeling were exposed
44 to 85% oxygen for postnatal day 1 (P1) - P14, while the control mice with normal lung
45 development were exposed to 21% oxygen. Male and female animals were used because no gender
46 bias was found in the study on perturbations to lung development of C57Bl/6J mice in response to
47 hyperoxia. The care dam was rotated every 24 h under normal hypoxia and hyperoxia in order to
48 limit oxygen toxicity. Mice in P3 (before the formation of large alveoli), P5 (peak of large alveolar
49 formation), or P14 (the stage of massive alveolarization) were euthanized by intraperitoneal
50
51
52
53
54
55
56
57
58
59
60
61
62
63
64
65

1 injection of excessive pentobarbital (500 mg/kg), and the lungs of mice were then extracted for
2 further analyses. The mice were then randomly assigned into the control group (normal air-treated
3 C57B1/6J newborn mice), the BPD group (hyperoxia-induced BPD mice), the BPD + HDAC3^{-/-}
4 group (BPD mice treated with HDAC3 knockout) [14], the hyperoxia + HDAC3^{-/-} + antagomir NC
5 group (hyperoxia-induced BPD mice with HDAC3 knockout and injected with antagomir NC), and
6 the hyperoxia + HDAC3^{-/-} + miR-17-antagomir group (hyperoxia-induced BPD mice with HDAC3
7 knockout and injected with miR-17-antagomir), with ten mice in each group.
8
9
10
11
12
13
14
15
16
17

18 **Cell culture and grouping**

19
20 Primary lung fibroblasts were isolated from C57B1/6J mice. Briefly, the lungs were injected with
21 approximately 500 μ L of preheated collagenase type I (2 mg/mL) at 37°C and then excised from
22 adult female C57BL/6J mice after euthanized by isoflurane inhalation. The lung tissues were then
23 placed in a 50 mL tube containing 25 mL of preheated collagenase type I and treated at 70 rpm for 1
24 h at 37°C using an orbital rotator (Unimax 1010) with gentle agitation. The lungs were then minced
25 using sterile scissors and the tissue suspension was dispersed by using a 20G syringe needle. The
26 cell suspension was then injected through a 40 mL filter into a new 50 mL tube, followed by
27 centrifugation at 120 g at 4°C for 8 min, with the supernatant discarded. The cell pellet was then
28 resuspended in preheated (37°C) high-glucose Dulbecco's modified Eagle's medium (DMEM)
29 containing 10% (v/v) fetal bovine serum (FBS), 100 U/mL penicillin (ThermoFisher Scientific,
30 Waltham, MA, USA) and 100 μ g/mL streptomycin (ThermoFisher Scientific), followed by
31 inoculation into a T-75 cell culture flask (1 flask per lung), then by passage in low-glucose DMEM
32 containing 10% (v/v) FBS, 100 U/mL penicillin, and 100 μ g/mL streptomycin. The cells used in
33 this study were primary isolated and cultured lung fibroblasts [15].
34
35
36
37
38
39
40
41
42
43
44
45
46
47
48
49
50
51
52
53

54 The lung fibroblasts were cultured in a 6-well plate at a cell concentration of 2×10^5 cells/per
55 tube. When the cells reached 80% confluence, transfection was performed according to the
56 manufacturer's instructions of the lipofectamine 2000 specifications (11668-019, Invitrogen, New
57
58
59
60
61
62
63
64
65

York, California, USA). The fibroblasts were transfected with following plasmids: short hairpin (sh) RNA-negative control (NC), sh-HDAC3, inhibitor-NC, miR-17-inhibitor, sh-HDAC3 + inhibitor-NC, sh-HDAC3 + miR-17-inhibitor, overexpressed (oe)-NC, oe-EZH1, sh-NC, sh-p65 and oe-EZH1 + sh-p65 (Guangzhou RiboBio Co., Ltd., Guangzhou, Guangdong, China). After 12 h of transfection, the cells were cultured for 48 h at 37°C under 5% CO₂ for subsequent RNA extraction and other relevant experiments.

Hematoxylin-eosin (HE) staining

The left lung tissues of mice in different groups were fixed in 10% neutral formaldehyde solution for more than 24 h, paraffin-embedded, dewaxed twice with xylene (10 min/time), then rehydrated with 100% ethanol for 5 min, 90% ethanol for 2 min, 70% ethanol for 2 min, washed with distilled water for 2 min and stained with hematoxylin for 7 min. After washing for 10 min with tap water to remove the excess dye solution, the samples were then washed with distilled water again and subsequently treated with 95% ethanol for 5 s, stained with eosin for 1 min, hydrated using gradient ethanol (100%, 95%, 75%, 50%, twice, 2 min/time), cleared twice by xylene (5 min/time), and air-dried. The lung tissues were then blocked with neutral resin in a fume hood and the morphological changes of lung tissues were observed under an optical microscope.

Immunohistochemistry

Left lung tissues were taken from the euthanized mice, fixed in 4% paraformaldehyde, embedded in paraffin, serially sectioned at a thickness of 4 μm and routinely dewaxed. The streptavidin-peroxidase (SP) method was routinely conducted. Briefly, antigen retrieval was performed by microwave heating. The sections were blocked by the addition of normal goat serum blocking solution. BPD group was used as a NC. The staining was conducted with the Histostain™ SP-9000 immunohistochemical staining kit (Zymed Laboratories Inc., South San Francisco, CA, USA). The sections were then probed at 4°C overnight with the following primary

antibodies purchased from Abcam Inc. (Cambridge, UK): rabbit anti-EZH1 (ab64850, 1: 100),
1 rabbit anti-NF- κ B p65 (ab16502, 1: 100), and rabbit anti-Pgf (ab230516, 1: 100). After rinsing with
2
3 PBS, the sections were immediately probed with mouse anti-rabbit secondary antibody (ab6728, 1:
4
5 1000, Abcam) at 37°C for 30 min. After PBS washing, the horseradish peroxidase (HRP)-labeled
6
7 working solution was added to the sections and incubated, followed by diaminobenzidine (DAB)
8
9 development for 5 to 10 min. The staining time was adjusted under a microscope and the sections
10
11 were sealed using gum after 1 min of hematoxylin counterstaining. Then, five representative
12
13 high-power fields were selected for cell observation and counting. The cytoplasm stained brown or
14
15 yellow were indicative of positive cells.
16
17
18
19
20
21
22

Immunofluorescence staining of microvessel density (MVD)

The lung tissue sections were deparaffinized, rehydrated, and stained with rabbit polyclonal
25
26 antibody to Von Willebrand Factor (vWF, ab11713, 1: 100, Abcam). The number of blood vessels
27
28 (20-50 μ m diameter) of each high power field (HPF) was counted in five randomly selected
29
30 non-overlapping parenchymal regions of the lung tissue sections of the animals (n = 6). The detailed
31
32 procedures were carried out as previously described [16].
33
34
35
36
37
38
39

Reverse transcription-quantitative polymerase chain reaction (RT-qPCR)

Lung fibroblasts in each group were collected and lysed using the TRIzol kit (Invitrogen). Then, the
42
43 total RNA was extracted from cells and tissue samples. The quality and concentration of RNA were
44
45 measured using an ultraviolet-visible spectrophotometer (ND-1000, Nanodrop, Wilmington, DE,
46
47 USA). An amount of 400 ng of the extracted RNA was subjected to reverse transcription by using a
48
49 PrimeScript RT Reagent Kit (Takara, Shiga, Japan). With complementary DNA (cDNA) as a
50
51 template, a fluorescent quantitative PCR was carried out in accordance with the manufacturer's
52
53 instructions of a SYBR® Premix Ex Taq™ II (Tli RNaseH Plus) kit (Takara). The primers were
54
55 synthesized by RiboBio Company and were shown in Table 1. Glyceraldehyde-3-phosphate
56
57
58
59
60
61
62
63
64
65

dehydrogenase (GAPDH) or U6 was used as a loading control gene. The fold changes were calculated using the relative quantification (the $2^{-\Delta\Delta Ct}$ method): $\Delta\Delta Ct = Ct_{(target\ gene)} - Ct_{(internal\ reference\ gene)}$.

Western blot analysis

Lung fibroblasts were washed with PBS, lysed with cell lysis buffer (C0481, Sigma-Aldrich, St. Louis, MO, USA) and incubated at 4°C for 30 min. Next, the cell lysate was collected into 1.5 mL Eppendorf tubes and centrifuged at 12,000 g at 4°C for 5 min, after which the supernatant was collected. The concentration of protein was measured using the bicinchoninic acid protein assay kit (Shanghai Beyotime Biotechnology Co. Ltd., Shanghai, China). Subsequently, 20 µg of protein was separated by 10% sodium dodecyl sulfate-polyacrylamide gel electrophoresis (SDS-PAGE) (Millipore, Billerica, MA, USA) and transferred onto a polyvinylidene fluoride membrane (Millipore). The membrane was then blocked with 5% skimmed milk powder for 1 h and probed with the following Tris-buffered saline Tween-20 (TBST) diluted primary antibodies purchased from Abcam: rabbit polyclonal antibody to HDAC3 (ab7030, 1: 1000), EZH1 (ab64850, 1: 250), p65 (ab19870, 1: 500) and Pgf (ab230516, 1: 1000) at 4°C overnight, followed by washing 3 times with TBST and then probed with HRP-labeled secondary antibody goat anti-mouse or goat anti-rabbit (HS101, 1: 1000; TransGen Biotech Co., Ltd., Beijing, China) at room temperature for 1 h. Following 6 rinses with TBST, the immunocomplexes on the membrane were visualized using an enhanced chemiluminescence kit (Shanghai Baoman Biotechnology Co., Ltd., Shanghai, China). With GAPDH (ab37168, 1: 1000, Abcam) as a loading control, the band intensities were quantified using Image J analysis software.

Chromatin immunoprecipitation (ChIP) assay

ChIP assay was used to detect the enrichment of HDAC3 in the promoter region of the miR-17-92 cluster and that of p65 in the Pgf promoter region using the EZ-Magna ChIP TMA kit (Millipore).

1 The lung fibroblasts of each group in logarithmic growth phase were cross-linked and cultured with
2 1% formaldehyde for 10 min, then terminated by adding 125 mM glycine at room temperature for 5
3 min. The cells were then washed twice with pre-chilled PBS and centrifuged at 2000 rpm for 5 min
4 after which the supernatant was collected. Next, the cells were resuspended in cell lysate [150 mM
5 Sodium chloride (NaCl), 50 mM Tris (pH 7.5), 5 mM ethylenediamine tetraacetic acid (EDTA),
6 0.005% NP40, 0.01% Triton X-100)] to prepare a final concentration of 2×10^6 cells/200 mL. The
7 cells were then added with protease inhibitor mixture, centrifuged at 5000 rpm for 5 min,
8 resuspended in nuclear separation buffer, lysed in ice water bath for 10 min and sonicated to obtain
9 a 200-1000 bp chromatin fragment. The supernatant was then aspirated following centrifugation at
10 14,000 g for 10 min at 4°C. Then, 100 μ L of the supernatant (DNA fragment) in each group was
11 collected and added with 900 μ L of CHIP Dilution Buffer, 20 μ L of $50 \times$ pseudoisocyanine (PIC)
12 and 60 μ L of ProteinA agarose/salmon sperm DNA, followed by mixing at 4°C for 1 h, allowed to
13 stand at 4°C for 10 min and centrifuged at 700 rpm for 1 min. The supernatant was then collected,
14 20 μ L of which was taken as the Input. In the experimental groups, the supernatant was separately
15 incubated with 1 μ L of rabbit anti-HDAC3 (ab7030, 1: 500, Abcam) and rabbit anti-p65 (ab19870,
16 1: 100, Abcam). The supernatant in the NC groups was incubated with 1 μ L of rabbit
17 anti-immunoglobulin G (IgG) (ab172730, Abcam) and each tube was added with 60 μ L of ProteinA
18 agarose/salmon sperm DNA and incubated at 4°C for 2 h. Following standing for 10 min, the
19 samples were centrifuged at 700 rpm for 1 min and the supernatant was discarded. The precipitate
20 was washed with 1 mL of low salt buffer, high salt buffer, LiCl solution, and Tris-EDTA (TE) buffer
21 (twice) respectively. Each tube was eluted twice with 250 μ L of CHIP Wash Buffer and
22 decrosslinked with 20 mL of 5 M NaCl, after which the DNA was recovered and the promoter
23 sequences of miR-17-92 and Pgf in the complex were quantified by RT-qPCR.
24
25
26
27
28
29
30
31
32
33
34
35
36
37
38
39
40
41
42
43
44
45
46
47
48
49
50
51
52
53
54
55
56

57 **Dual-luciferase reporter gene assay**

58
59
60
61
62
63
64
65

1 The constructed 3' untranslated region (3'UTR) luciferase vector of EZH1 was cloned into the
2 pMIR reporter plasmid by PCR amplification of the potential binding site. For dual-luciferase
3 reporter gene assay, based on Lipofectamine 2000 (Invitrogen), lung fibroblasts containing the
4 EZH1 3'UTR and miR-17-5p mimics and inhibitors were transiently transfected into the pMIR
5 reporter vector. After 48 h of transfection, reporter gene activity was measured using a
6 dual-luciferase assay system (Promega, Madison, WI, USA). Renilla luciferase activity was used to
7 normalize transfection efficiency. The promoter activity of HDAC for miR-17-92 cluster was
8 described previously [14]. The effect of p65 on the promoter activity of Pgf was described
9 previously [17].
10
11
12
13
14
15
16
17
18
19
20
21
22

23 **Statistical analysis**

24
25 Statistical analyses were conducted using SPSS 21.0 software (IBM Corp. Armonk, NY, USA).
26 Measurement data were expressed as mean \pm standard deviation. Confirming to normal distribution
27 and homogeneity of variance, the data between two groups with the unpaired design were compared
28 using unpaired *t*-test. Data among multiple groups were analyzed by one-way analysis of variance
29 (ANOVA), followed by a Tukey's post-hoc test. The difference in *p*-value of $p < 0.05$ was
30 considered as statistically significant.
31
32
33
34
35
36
37
38
39
40
41

42 **Results**

43 **HDAC3 was involved in the regulation of BPD**

44
45 Previous literature has reported that HDAC3 was participated in the remodeling and expansion of
46 distant alveolar vesicles into primitive pulmonary alveolus by regulating the miR-17-92 cluster [14],
47 which commonly constitutes to the occurrence of BPD in premature infants [15]. Based on the
48 aforementioned evidence, it was suggested that HDAC3 may be involved in the progression of BPD.
49 Therefore, the molecular mechanism of HDAC3 involved in BPD was explored by establishing a
50 hyperoxia-induced mouse model of BPD. The degree of lung injury in mice was firstly evaluated by
51
52
53
54
55
56
57
58
59
60
61
62
63
64
65

1 HE staining. The results showed that the degree of lung injury in the BPD mice was notably higher
2 than that in the control mice (Fig. 1A). The degree of alveolarization in BPD mice was subsequently
3 examined and the results showed that the mean linear intercept (MLI) of alveoli in BPD mice was
4 significantly higher than that of the control mice, while the number of alveoli was less than that of
5 the control mice (Fig. 1B). Furthermore, the MVD in lung tissues was examined by
6 immunofluorescence assay, and the results suggested that the MVD of BPD mice was significantly
7 lower than that of the control mice (Fig. 1C). The expression of HDAC3 in lung tissues of BPD
8 mice was assessed by Western blot analysis, which demonstrated that the expression of HDAC3 in
9 lung tissues of BPD mice was markedly higher than that of control mice (Fig. 1D). Next, the
10 HDAC3 gene was knocked out in BPD mice, and it was verified that the degree of lung injury in
11 BPD + HDAC3^{-/-} mice was significantly reduced (Fig. 1A), the degree of alveolarization was
12 notably lower (Fig. 1B), as well as the MVD was higher when compared to BPD mice (Fig. 1C).
13 The expression of HDAC3 in lung tissues of BPD + HDAC3^{-/-} mice was also significantly lower
14 than that in the BPD mice as detected by Western blot analysis (Fig. 1D). These results
15 demonstrated that HDAC3 was involved in the regulation of alveolarization and angiogenesis in
16 BPD.
17
18
19
20
21
22
23
24
25
26
27
28
29
30
31
32
33
34
35
36
37
38
39

40 **HDAC3 inhibits the expression of miR-17-92 cluster in BPD**

41
42 RT-qPCR was used to detect the expression of miR-17-92 cluster (miR-17, miR-18a, miR-19a,
43 miR-19b, miR-20a, miR-92) in control mice, BPD mice and BPD + HDAC3^{-/-} mice. The results
44 showed that the expression of the miR-17-92 cluster in BPD mice was significantly lower than that
45 in control mice, but demonstrated increased expression of miR-17-92 cluster after HDAC3
46 knockout (Fig. 2A). Furthermore, the primary lung fibroblasts were isolated from BPD mice and
47 stably transfected with sh-NC and sh-HDAC3. The protein level of HDAC3 was detected by
48 western blot analysis. Results demonstrated that the protein level of HDAC3 was notably decreased
49 following silencing of HDAC3 expression (Fig. 2B). The expression of miR-17-92 cluster was then
50
51
52
53
54
55
56
57
58
59
60
61
62
63
64
65

1 detected in the cells, and the results indicated that the expression of miR-17-92 cluster in
2 sh-HDAC3-treated cells was markedly higher than those of sh-NC-treated cells (Fig. 2C), implying
3 that HDAC3 may regulate miR-17-92 cluster in BPD. To further elucidate the enrichment of
4 HDAC3 in the promoter region of miR-17-92 cluster, ChIP assay showed that HDAC3 was
5 enriched in the miR-17-92 cluster promoter, while silencing of HDAC3 resulted in the opposite
6 trend (Fig. 2D). Furthermore, the effect of HDAC3 on the luciferase activity of miR-17-92
7 promoter was examined by dual-luciferase reporter gene assay. The results showed that silencing of
8 HDAC3 expression resulted in inhibited luciferase activity of miR-17-92 promoter (Fig. 2E). Based
9 on the aforementioned results, it was suggested that HDAC3 could regulate the expression of
10 miR-17-92 cluster in BPD.
11
12
13
14
15
16
17
18
19
20
21
22
23
24

25 **EZH1 was a target gene of miR-17 in miR-17-92 cluster**

26
27 To further explore the underlying mechanism of miR-17 in the miR-17-92 cluster in the regulation
28 of BPD, the Targetscan website was employed to predict whether miR-17 could bind to EZH1. It
29 was verified that miR-17 could bind to EZH1 (Fig. 3A). Previous study has been reported that
30 miR-17 could be involved in the regulation of drug resistance in non-small cell lung cancer *via*
31 targeting and regulating EZH1 expression [11]. To further explore the regulatory mechanism of
32 miR-17 and EZH1 in alveolarization, lung fibroblasts were stably transfected with inhibited and
33 overexpressed miR-17 in BPD. RT-qPCR was performed to detect miR-17 expression in cells, and
34 the results showed that inhibited miR-17 resulted in decreased miR-17 expression, while
35 overexpression of miR-17 resulted in increased miR-17 expression (Fig. 3B). The binding of
36 miR-17 to EZH1 was then examined by a dual-luciferase reporter gene assay, and the results
37 revealed that overexpression of miR-17 resulted in inhibited luciferase activity of EZH1 3'UTR,
38 while suppression of miR-17 resulted in promoted luciferase activity of EZH1 3'UTR (Fig. 3C).
39 Results from RT-qPCR and Western blot analysis demonstrated that overexpressed miR-17 resulted
40 in inhibited EZH1 expression, whereas inhibited miR-17 resulted in promoted EZH1 expression
41
42
43
44
45
46
47
48
49
50
51
52
53
54
55
56
57
58
59
60
61
62
63
64
65

(Fig. 3D). To further investigate whether HDAC3 could affect EZH1 expression through miR-17 in lung fibroblasts in BPD, the expression of EZH1 in fibroblasts transfected with sh-HDAC3, or with both HDAC3 silencing and miR-17 inhibitor was examined. The results verified that the expression of EZH1 was inhibited by silencing of HDAC3 expression, but it could be restored by the co-transfection of HDAC3 silencing and miR-17 inhibitor (Fig. 3E). The above results showed that miR-17 was involved in the regulation of EZH1 by modulating HDAC3 in BPD.

EZH1 activates p65 transcription factor to enhance Pgf expression

According to previous literature, EZH1 could bind to p65 transcription factor to promote the transcription of downstream target genes [11], while in human Pgf promoter region, p65 has been reported to bind directly to the promoter region of Pgf/Plgf and transcriptionally activates Pgf/Plgf [12]. Pgf has been demonstrated to be involved in the regulation of BPD [13]. Therefore, it was hypothesized that EZH1 may promote p65 to activate the transcription of Pgf in BPD mice. Initially, the binding sites of p65 and Pgf were obtained (Fig. 4A). The expression of EZH1 in fibroblasts transfected with oe-EZH1 was detected by RT-qPCR and Western blot analysis. It was shown that the expression of EZH1 was significantly up-regulated after the transfection with oe-EZH1 in fibroblasts of BPD mice (Fig. 4B). The binding of EZH1 to p65 was further examined by immunoprecipitation (IP) assay, and the results showed that the overexpression of EZH1 promoted the binding of EZH1 to p65 (Fig. 4C). Besides, results from the ChIP assay revealed that the overexpression of EZH1 promoted the enrichment of p65 in the Pgf promoter region (Fig. 4D). The non-fibroblasts of BPD mice that stably transfected with silencing of p65 were constructed and the expression of p65 was detected. The results showed that silencing of p65 expression resulted in inhibited expression of p65 in non-fibroblasts of BPD mice (Fig. 4E). The expression of Pgf was then detected in silencing p65-treated cells, and the results suggested that silencing of p65 expression resulted in inhibited expression of Pgf (Fig. 4F). Moreover, it has been indicated that EZH1 may be involved in the regulation of Pgf expression. Next, Pgf expression was detected in

oe-EZH1-treated cells. The overexpression of EZH1 resulted in promoted Pgf expression, and the expression of Pgf was rescued in cells after co-transfection of sh-p65 and oe-EZH1 (Fig. 4G). The above-mentioned data indicated that EZH1 could participate in the regulation of BPD by recruiting p65 to promote Pgf expression.

HDAC3 regulates Pgf expression via miR-17-EZH1-p65 axis

To further explore the regulatory role of HDAC3 on Pgf expression in BPD, the expression of Pgf was initially assessed by RT-qPCR and western blot analysis in cells transfected with silencing of HDAC3 expression and inhibited miR-17. The corresponding results suggested that the silencing of miR-17 resulted in promoted Pgf expression, whereas silencing of HDAC3 resulted in inhibited Pgf expression, while Pgf expression was rescued in cells after co-transfection of sh-HDAC3 and miR-17 inhibitor (Fig. 5A). According to our previous results, HDAC3 regulated the expression of EZH1 through miR-17, therefore it was hypothesized that HDAC3 could promote the transcription of Pgf via miR-17-EZH1-p65 axis. CHIP assay was used to detect the enrichment of p65 in the Pgf promoter region in cells transfected with sh-HDAC3, miR-17 inhibitor, or both. The results showed that silencing of HDAC3 inhibited the enrichment of p65 in the Pgf promoter region while silencing of miR-17 promoted the enrichment of p65 in the Pgf promoter region. Besides, the co-transfection of sh-HDAC3 and miR-17 inhibitor relatively restored the enrichment of p65 in the Pgf promoter region (Fig. 5B). These results demonstrated that HDAC3 could enhance the transcription and expression of Pgf via miR-17-regulated EZH1 and subsequently promote the recruitment of p65 in the Pgf promoter region.

HDAC3 regulates Pgf via miR-17 in miR-17-92 cluster and promotes BPD development

To further demonstrate the regulatory role of HDAC3 on Pgf in BPD mice via the miR-17-EZH1-p65 axis *in vivo*, hyperoxia + HDAC3^{-/-} + miR-17-antagomir mice were constructed through injection of miR-17 antagomir into hyperoxia + HDAC3^{-/-} mice. The expression of miR-17

in mice following different treatment was initially detected by RT-qPCR. The results showed that miR-17 expression in hyperoxia + HDAC3^{-/-} mice was significantly higher than that in hyperoxia-induced BPD mice, but relatively decreased in hyperoxia + HDAC3^{-/-} + miR-17-antagomir-treated mice, which was similar to that in the BPD mice (Fig. 6A). Furthermore, the degree of lung injury in mice was detected by HE staining. It was demonstrated that the degree of lung injury in hyperoxia + HDAC3^{-/-}-treated mice was notably improved when compared to the hyperoxia-induced BPD mice. The degree of lung injury in hyperoxia + HDAC3^{-/-} + miR-17-antagomir-treated mice was similar to that in the hyperoxia-induced BPD mice (Fig. 6B). The alveolar number and MLI of the mice were subsequently detected to evaluate the degree of alveolarization in mice. Results demonstrated that the MLI of hyperoxia + HDAC3^{-/-} mice-treated was significantly reduced, and that of the MLI of hyperoxia + HDAC3^{-/-} + miR-17-antagomir mice was similar to that of hyperoxia-induced BPD mice (Fig. 6C). The number of alveolar in hyperoxia + HDAC3^{-/-}-treated mice was notably higher than that in the BPD mice, and the number of alveoli in hyperoxia + HDAC3^{-/-}+ miR-17-antagomir-treated mice was similar to that in the hyperoxia-induced BPD mice (Fig. 6D). The MVD of lung tissue in each group was detected by immunofluorescence assay. It was shown that the MVD of hyperoxia + HDAC3^{-/-}-treated mice was markedly higher than that of BPD mice, and the MVD of hyperoxia + HDAC3^{-/-} + miR-17-antagomir-treated mice was similar to that of the hyperoxia-induced BPD mice (Fig. 6E). Besides, it was shown that HDAC3 could regulate the alveolarization and angiogenesis *via* miR-17 in BPD mice. Furthermore, the expression of EZH1, p65, and Pgf in lung tissue of mice in different groups was examined by immunohistochemistry. The results showed that the expression of EZH1, p65, and Pgf in hyperoxia + HDAC3^{-/-}-treated mice was significantly lower than that in BPD mice, whereas the expression of EZH1, p65, and Pgf in hyperoxia + HDAC3^{-/-} + miR-17-antagomir-treated mice was similar to the hyperoxia-induced BPD mice (Fig. 6F). The above-mentioned results demonstrated that HDAC3 could regulate Pgf expression through the miR-17-EZH1-p65 axis to participate in alveolarization and pulmonary angiogenesis of BPD mice.

Discussion

Bronchopulmonary dysplasia (BPD) is a serious complication afflicting preterm infants which arises from oxygen toxicity and mechanical injury during oxygen supplementation [18]. Despite significant advances in the treatment of BPD, the mortality and morbidity of patients with BPD still very high, and yet the underlying mechanism of BPD progression remains poorly understood and inadequately defined [19]. Therefore, the discovery of therapeutic targets is critically needed to facilitate the diagnosis and treatment of patients with BPD. Existing literature has highlighted the participation of HDAC in various pathological and physiological processes including BPD [5]. In this study, we established *in vivo* BPD mouse models and identified that HDAC3 might be an endogenous regulator of BPD, as HDAC3 could promote the angiogenesis and alveolarization in BPD by enhancing Pgf *via* the miR-17-EZH1-p65 axis.

Initial results revealed that the expression of HDAC3 was highly expressed while the miR-17-92 cluster was poorly expressed in BPD mice. As one of the members in the class I histone deacetylase family, HDAC3 possesses regulatory function on gene expression through the deacetylation of both histones and non-histone proteins [20]. HDAC3 has been shown to be upregulated in adenocarcinoma of the lung, which was related to its poor prognosis [6]. In agreement with our findings, the expression of miR-17 in the miR-17-92 cluster has been found to be poorly expressed in infants diagnosed with severe BPD, and also was correlated with the diagnosis of BPD [21]. Previous evidence has shown that HDAC3 could participate in regulating the remodeling and expansion of distant alveolar vesicles into primitive lung alveologenesis through mediation of miR-17-92 cluster [14], suggesting that HDAC3 may exert a regulatory role in the angiogenesis and alveolarization of BPD through inhibiting the expression of miR-17-92 cluster.

Next, the results obtained from dual-luciferase reporter gene assay indicated that miR-17 could bind to the 3'-UTR of EZH1, demonstrating that EZH1 was a target gene of miR-17 and could be negatively regulated by miR-17. EZH1, a component of polycomb repressive complex 2, has been

1 demonstrated to exert a significant role in repressing the transcription of target genes that affect the
2 pathogenesis of various diseases [22]. The interaction between miRNA and its target mRNAs and
3 their functional mechanisms in the pathophysiology of BPD have been addressed [23]. EZH1 has
4 been previously reported to be a target gene of miR-17-5p, and the down-regulation of miR-17-5p
5 could enhance the resistance to erlotinib in non-small cell lung cancer by regulating EZH1 [24],
6 which was in consistent with our experimental results whereby miR-17 in the miR-17-92 cluster
7 negatively regulated EZH1 expression, which reflects the biological characteristics of BPD.
8
9

10 Subsequently, we found out that EZH1 could promote Pgf expression by recruiting p65 and
11 then participated in the regulation of BPD. As an important molecule in angiogenesis, Pgf/Plgf has a
12 regulatory effect on pathological conditions including tumor formation, ischemia, cardiovascular
13 diseases, suggesting that it may serve as a novel therapeutic target in various diseases [25].
14 Moreover, Pgf has an essential role in pulmonary vascular development of BPD [26]. According to
15 previous literature, it was demonstrated that EZH1 could mediate the recruitment of p65 to promote
16 the transcription of target genes [11]. In addition, p65 could directly bind to the Pgf promoter region,
17 leading to a substantial activation of Pgf transcript levels [12]. These results were in line with our
18 results and the interaction of EZH1, p65 and Pgf in regulating the angiogenesis and alveolarization
19 of BPD were verified. Another important finding was that HDAC3 could stimulate Pgf expression
20 *via* the miR-17-EZH1-p65 axis, thus promoting the progression of BPD.
21
22
23
24
25
26
27
28
29
30
31
32
33
34
35
36
37
38
39
40
41
42
43
44

45 Conclusions

46 In conclusion, the key findings obtained from the current study was the identification of the
47 regulatory role of HDAC3 interacting with the miR-17-EZH1-p65-Pgf axis in pulmonary
48 angiogenesis and alveolarization in newborn mice with BPD (Fig. 7). The upregulation of HDAC3
49 and inhibition of miR-17 expression were observed in BPD mice. In addition, the binding of
50 miR-17 to EZH1 could regulate the recruitment of p65 to enhance the transcription of target gene
51 Pgf, thereby regulating BPD. These findings suggest that HDAC3 may serve as a promising
52
53
54
55
56
57
58
59
60
61
62
63
64
65

diagnostic biomarker and therapeutic target for BPD. At present, the effects and mechanisms of
HDAC3 interacting with miR-17-EZH1-p65-Pgf in BPD remain scanty identified. Therefore, more
in-depth investigation is urgently needed to further discuss the underlying rules that govern their
interaction, which might increase the feasibility and safety of its therapy in clinical applications.

1
2
3
4
5
6
7
8
9
10
11
12
13
14
15
16
17
18
19
20
21
22
23
24
25
26
27
28
29
30
31
32
33
34
35
36
37
38
39
40
41
42
43
44
45
46
47
48
49
50
51
52
53
54
55
56
57
58
59
60
61
62
63
64
65

Abbreviations

1 BPD, Bronchopulmonary dysplasia; HDACs, Histone deacetylases; miR, microRNA; FBS, fetal
2 bovine serum; HE, Hematoxylin-eosin; SP, streptavidin-peroxidase; MVD, microvessel density;
3
4 RT-qPCR, Reverse transcription-quantitative polymerase chain reaction; cDNA, complementary
5
6 DNA; GAPDH, Glyceraldehyde-3-phosphate dehydrogenase; TBST, Tris-buffered saline Tween-20;
7
8 SDS-PAGE, sodium dodecyl sulfate-polyacrylamide gel electrophoresis; ChIP, Chromatin
9
10 immunoprecipitation; assay NaCl, Sodium chloride; EDTA, ethylenediamine tetraacetic acid; PIC,
11
12 pseudoisocyanine; IgG, immunoglobulin G; 3'UTR, 3' untranslated region; ANOVA, analysis of
13
14 variance.
15
16
17
18
19
20
21
22

Declarations

Author contributions

23
24
25
26
27
28
29
30 DW, HH, and XXL designed the study, and were involved in data collection. DW and JL performed
31
32 the statistical analysis and preparation of figures. HH and ZQZ drafted the paper. All authors read
33
34 and approved the final manuscript.
35
36
37
38
39
40

Funding

41
42
43
44 This work was supported by Zhejiang Provincial Natural Science Foundation of China (Grant
45
46 Number: LY20H040008, LGF20H020004).
47
48
49
50

Availability of data and materials

51
52
53
54 Data generated and analyzed as part of this study are included in the manuscript or are available
55
56 upon request from the corresponding author.
57
58
59
60
61
62
63
64
65

Ethics approval and consent to participate

1
2 All animal experiments were conducted in strict accordance with the Guide to the Management and
3
4 Use of Laboratory Animals issued by the National Institutes of Health. The protocol of animal
5
6 experiments was approved by the Institutional Animal Care and Use Committee of Affiliated
7
8 Hangzhou First People's Hospital, Zhejiang University School of Medicine.
9

Consent for publication

10
11
12
13
14
15
16
17 Not applicable
18
19
20

Competing interests

21
22
23
24
25 The authors declare that they have no competing interests.
26
27
28

Acknowledgement

29
30
31
32 The authors sincerely appreciate all members participated in this work.
33
34
35
36
37
38
39
40
41
42
43
44
45
46
47
48
49
50
51
52
53
54
55
56
57
58
59
60
61
62
63
64
65

References

1. Gallini F, Arena R, Stella G, Frezza S, Maggio L: **Neurodevelopmental outcomes of premature infants with bronchopulmonary dysplasia.** *Acta Biomed* 2014, **85**: 30-34.
2. Thebaud B, Abman SH: **Bronchopulmonary dysplasia: where have all the vessels gone? Roles of angiogenic growth factors in chronic lung disease.** *Am J Respir Crit Care Med* 2007, **175**: 978-985.
3. Niedermaier S, Hilgendorff A: **Bronchopulmonary dysplasia - an overview about pathophysiologic concepts.** *Mol Cell Pediatr* 2015, **2**: 2.
4. Davidson LM, Berkelhamer SK: **Bronchopulmonary Dysplasia: Chronic Lung Disease of Infancy and Long-Term Pulmonary Outcomes.** *J Clin Med* 2017, **6**:
5. Cantley MD, Zannettino ACW, Bartold PM, Fairlie DP, Haynes DR: **Histone deacetylases (HDAC) in physiological and pathological bone remodelling.** *Bone* 2017, **95**: 162-174.
6. Minamiya Y, Ono T, Saito H, Takahashi N, Ito M, Motoyama S, Ogawa J: **Strong expression of HDAC3 correlates with a poor prognosis in patients with adenocarcinoma of the lung.** *Tumour Biol* 2010, **31**: 533-539.
7. Park D, Park H, Kim Y, Kim H, Jeoung D: **HDAC3 acts as a negative regulator of angiogenesis.** *BMB Rep* 2014, **47**: 227-232.
8. Chen CQ, Chen CS, Chen JJ, Zhou LP, Xu HL, Jin WW, Wu JB, Gao SM: **Histone deacetylases inhibitor trichostatin A increases the expression of Dleu2/miR-15a/16-1 via HDAC3 in non-small cell lung cancer.** *Mol Cell Biochem* 2013, **383**: 137-148.
9. Singh RP, Massachi I, Manickavel S, Singh S, Rao NP, Hasan S, Mc Curdy DK, Sharma S, Wong D, Hahn BH, Rehimi H: **The role of miRNA in inflammation and autoimmunity.** *Autoimmun Rev* 2013, **12**: 1160-1165.
10. Rogers LK, Robbins M, Dakhllallah D, Yang Z, Lee LJ, Mikhail M, Nuovo G, Pryhuber GS, McGwin G, Marsh CB, Tipple TE: **Attenuation of miR-17 approximately 92 Cluster in Bronchopulmonary Dysplasia.** *Ann Am Thorac Soc* 2015, **12**: 1506-1513.
11. Su SK, Li CY, Lei PJ, Wang X, Zhao QY, Cai Y, Wang Z, Li L, Wu M: **The EZH1-SUZ12 complex positively regulates the transcription of NF-kappaB target genes through interaction with UXT.** *J Cell Sci* 2016, **129**: 2343-2353.
12. Cramer M, Nagy I, Murphy BJ, Gassmann M, Hottiger MO, Georgiev O, Schaffner W: **NF-kappaB contributes to transcription of placenta growth factor and interacts with metal responsive transcription factor-1 in hypoxic human cells.** *Biol Chem* 2005, **386**: 865-872.
13. Janer J, Andersson S, Haglund C, Karikoski R, Lassus P: **Placental growth factor and vascular endothelial growth factor receptor-2 in human lung development.** *Pediatrics* 2008, **122**: 340-346.
14. Wang Y, Frank DB, Morley MP, Zhou S, Wang X, Lu MM, Lazar MA, Morrisey EE: **HDAC3-Dependent Epigenetic Pathway Controls Lung Alveolar Epithelial Cell Remodeling and Spreading via miR-17-92 and TGF-beta Signaling Regulation.** *Dev Cell* 2016, **36**: 303-315.
15. Ruiz-Camp J, Quantius J, Lignelli E, Arndt PF, Palumbo F, Nardiello C, Surate Solaligue DE, Sakkas E, Mizikova I, Rodriguez-Castillo JA, Vadasz I, Richardson WD, Ahlbrecht K, Herold S, Seeger W, Morty RE: **Targeting miR-34a/Pdgfra interactions partially corrects alveologenesis in experimental bronchopulmonary dysplasia.** *EMBO Mol Med* 2019, **11**:
16. Reiter J, Drummond S, Sammour I, Huang J, Florea V, Dornas P, Hare JM, Rodrigues CO, Young KC: **Stromal derived factor-1 mediates the lung regenerative effects of mesenchymal stem cells in a rodent model of bronchopulmonary dysplasia.** *Respir Res* 2017, **18**: 137.
17. Chaballe L, Close P, Sempels M, Delstanche S, Fanielle J, Moons L, Carmeliet P, Schoenen J, Chariot A, Franzen R: **Involvement of placental growth factor in Wallerian degeneration.** *Glia* 2011, **59**: 379-396.
18. Jobe AH: **Mechanisms of Lung Injury and Bronchopulmonary Dysplasia.** *Am J Perinatol* 2016, **33**: 1076-1078.
19. Higgins RD, Jobe AH, Koso-Thomas M, Bancalari E, Viscardi RM, Hartert TV, Ryan RM, Kallapur SG, Steinhorn RH, Konduri GG, Davis SD, Thebaud B, Clyman RI, Collaco JM, Martin CR, Woods JC, Finer NN, Raju TNK: **Bronchopulmonary Dysplasia: Executive Summary of a Workshop.** *J Pediatr* 2018, **197**: 300-308.
20. Chini CC, Escande C, Nin V, Chini EN: **HDAC3 is negatively regulated by the nuclear protein DBC1.** *J Biol Chem* 2010, **285**: 40830-40837.
21. Robbins ME, Dakhllallah D, Marsh CB, Rogers LK, Tipple TE: **Of mice and men: correlations between microRNA-17 approximately 92 cluster expression and promoter methylation in severe bronchopulmonary dysplasia.** *Am J Physiol Lung Cell Mol Physiol* 2016, **311**: L981-L984.
22. Rizq O, Mimura N, Oshima M, Saraya A, Koide S, Kato Y, Aoyama K, Nakajima-Takagi Y, Wang C, Chiba T, Ma A, Jin J, Iseki T, Nakaseko C, Iwama A: **Dual Inhibition of EZH2 and EZH1 Sensitizes PRC2-Dependent Tumors to Proteasome Inhibition.** *Clin Cancer Res* 2017, **23**: 4817-4830.
23. Dong J, Carey WA, Abel S, Collura C, Jiang G, Tomaszek S, Sutor S, Roden AC, Asmann YW, Prakash YS, Wigle DA: **MicroRNA-mRNA interactions in a murine model of hyperoxia-induced bronchopulmonary dysplasia.** *BMC Genomics* 2012, **13**: 204.
24. Zhang W, Lin J, Wang P, Sun J: **miR-17-5p down-regulation contributes to erlotinib resistance in non-small**

cell lung cancer cells. *J Drug Target* 2017, **25**: 125-131.

25. Sorice R, Ruggiero D, Nutile T, Aversano M, Husemoen L, Linneberg A, Bourgain C, Leutenegger AL, Ciullo M: **Genetic and environmental factors influencing the Placental Growth Factor (PGF) variation in two populations.** *PLoS One* 2012, **7**: e42537.
26. Procianoy RS, Hentges CR, Silveira RC: **Vascular Endothelial Growth Factor/Placental Growth Factor Heterodimer Levels in Preterm Infants with Bronchopulmonary Dysplasia.** *Am J Perinatol* 2016, **33**: 480-485.

1
2
3
4
5
6
7
8
9
10
11
12
13
14
15
16
17
18
19
20
21
22
23
24
25
26
27
28
29
30
31
32
33
34
35
36
37
38
39
40
41
42
43
44
45
46
47
48
49
50
51
52
53
54
55
56
57
58
59
60
61
62
63
64
65

Figure legends

1
2 **Fig. 1** HDAC3 is implicated in the regulation of alveolarization and angiogenesis in BPD. A, The
3
4 degree of lung injury of mice in each group detected by HE staining ($\times 400$). B, The degree of
5
6 alveolarization and MLI of alveoli in BPD mice. C, MVD in lung tissues of mice in each group
7
8 assessed by immunofluorescence assay ($\times 200$). D, HDAC3 protein expression in lung tissues of
9
10 mice in each group detected by Western blot analysis. * $p < 0.05$. The above data were measurement
11
12 data and expressed as mean \pm standard deviation. Data among multiple groups were analyzed by
13
14 one-way ANOVA, followed by Tukey's post-hoc test. $n = 10$ for each mouse group.
15
16

17
18 **Fig. 2** HDAC3 suppresses the expression of the miR-17-92 cluster in BPD. A, The expression of
19
20 miR-17-92 cluster in lung tissues of different groups of mice detected by RT-qPCR. B, Western blot
21
22 analysis of HDAC3 protein expression after silencing of HDAC3 expression. C, The expression of
23
24 miR-17-92 cluster in cells following HDAC3 silencing detected by RT-qPCR. D, The enrichment of
25
26 HDAC3 in the promoter region of miR-17-92 cluster in cells following different transfection. E:
27
28 Luciferase activity of miR-17-92 cluster promoter detected by dual-luciferase reporter gene assay. *
29
30 $p < 0.05$. The above data were measurement data and expressed as mean \pm standard deviation. Data
31
32 among multiple groups were analyzed by one-way ANOVA, followed by Tukey's post-hoc test. $n =$
33
34
35
36
37
38
39
40
41
42
43
44
45
46
47
48
49
50
51
52
53
54
55
56
57
58
59
60
61
62
63
64
65

60
61 **Fig. 3** miR-17 in the miR-17-92 cluster targets EZH1 and regulates its expression in primary lung
62
63 fibroblasts of BPD mice. A, The binding site of miR-17 and EZH1 predicted by Targetscan website.
64
65 B, The expression of miR-17 in cells transfected with miR-17 mimic and miR-17 inhibitor detected
66
67 by RT-qPCR. C, The binding of miR-17 to EZH1 detected by dual-luciferase reporter gene assay. D,
68
69 The expression of EZH1 in cells transfected with miR-17 mimic and miR-17 inhibitor detected by
70
71 RT-qPCR and Western blot analysis. E, The expression of EZH1 in fibroblasts transfected with
72
73 HDAC3 silencing, or both HDAC3 silencing and miR-17 inhibitor detected by RT-qPCR and
74
75 Western blot analysis. * $p < 0.05$. The above data were measurement data and expressed as mean \pm
76
77 standard deviation. Data among multiple groups were analyzed by one-way ANOVA, followed by
78
79
80
81
82
83
84
85
86
87
88
89
90
91
92
93
94
95
96
97
98
99
100

Tukey's post-hoc test. n = 10 for each mouse group.

1 **Fig. 4** EZH1 promotes the expression of Pgf *via* p65 transcription factor stimulation. A, The binding
2 sites between p65 and Pgf. B, The expression of EZH1 in cells transfected with oe-EZH1 detected
3 by RT-qPCR and Western blot analysis. C, The binding of EZH1 and p65 detected by IP assay. D,
4 The enrichment of p65 in the Pgf promoter region in oe-EZH1-treated cells detected by ChIP assay.
5 E, The expression of p65 in p65 silencing-treated cells detected by Western blot analysis. F, The
6 expression of Pgf in p65 silencing-treated cells detected by RT-qPCR and Western blot analysis. G,
7 The expression of Pgf in fibroblasts transfected with oe-EZH1, or both oe-EZH1 and sh-p65
8 detected by RT-qPCR and Western blot analysis. * $p < 0.05$. The above data were measurement data
9 and expressed as mean \pm standard deviation. The data between the two groups with unpaired design
10 were compared by unpaired *t*-test. Data among multiple groups were analyzed by one-way ANOVA,
11 followed by Tukey's post-hoc test. n = 10 for each mouse group.
12
13
14
15
16
17
18
19
20
21
22
23
24
25
26

27 **Fig. 5** HDAC3 potentiates the transcription and the expression of Pgf *via* the miR-17-EZH1-p65
28 axis. A, The expression of Pgf detected by RT-qPCR and Western blot analysis. B, The enrichment
29 of p65 in Pgf promoter region detected by ChIP assay. * $p < 0.05$. The above data were
30 measurement data and expressed as mean \pm standard deviation. Data among multiple groups were
31 analyzed by one-way ANOVA, followed by Tukey's post-hoc test. n = 10 for each mouse group.
32
33
34
35
36
37
38
39

40 **Fig. 6** HDAC3 regulates Pgf expression through miR-17 to promote the alveolarization and
41 pulmonary angiogenesis of BPD. A, The expression of miR-17 in different groups of mice detected
42 by RT-qPCR. B, The degree of lung injury in mice of different groups detected by HE staining (\times
43 400). C: The MLI of alveolar in the lung tissue of mice in each group. D, The changes in alveolar
44 number in lung tissue of mice in each group. E, Immunofluorescence assay of MVD in lung tissues
45 of mice in each group ($\times 200$). F, The expression of EZH1, p65, and Pgf in lung tissues of mice
46 following different treatment detected by immunohistochemistry ($\times 400$). * $p < 0.05$. The above
47 data were measurement data and expressed as mean \pm standard deviation. Data among multiple
48 groups were analyzed by one-way ANOVA, followed by Tukey's post-hoc test. n = 10 for each
49
50
51
52
53
54
55
56
57
58
59
60
61
62
63
64
65

mouse group.

1 **Fig. 7** Schematic diagram depicting the role of HDAC3 regulating the miR-17-EZH1-p65-Pgf axis
2
3 in BPD in neonatal mice. HDAC3 was highly expressed in lung fibroblasts of BPD mice, inhibiting
4
5 the expression of miR-17 in the miR-17-92 cluster. miR-17 bound to EZH1 and regulated the
6
7 transcription and expression of Pgf, a downstream target gene of transcription factor p65 and
8
9 thereby regulating the development of BPD.
10
11
12
13
14
15
16
17
18
19
20
21
22
23
24
25
26
27
28
29
30
31
32
33
34
35
36
37
38
39
40
41
42
43
44
45
46
47
48
49
50
51
52
53
54
55
56
57
58
59
60
61
62
63
64
65

Table 1 Primer sequences for RT-qPCR

Target	Primer sequence (5'-3')
miR-17-92	F: TGAGGGCACTTGTAGCATTATG
	R: CCTTAGAACAAAAAGCACGCAG
miR-17-5p	F: GCGAATTCCAAATTTAGCAGGAATAAAG
	R: CGCTCGAGGACTGGACGCAGCCAGTG
Pgf	F: TTCCCCTTGGTTTTTCCTCCTT
	R: AGATCTTGAAGATTCCCCCCA
GAPDH	F: AAATGGTGAAGGTCGGTGTGAACG
	R: ATCTCCACTTTGCCACTGC
U6	F: GAACCTCACCTTGGGACTGA
	R: TGCTACAAGTGCCCTCACTG

F, forward; R, reverse

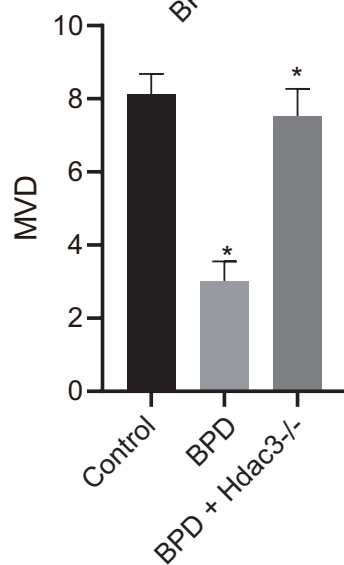
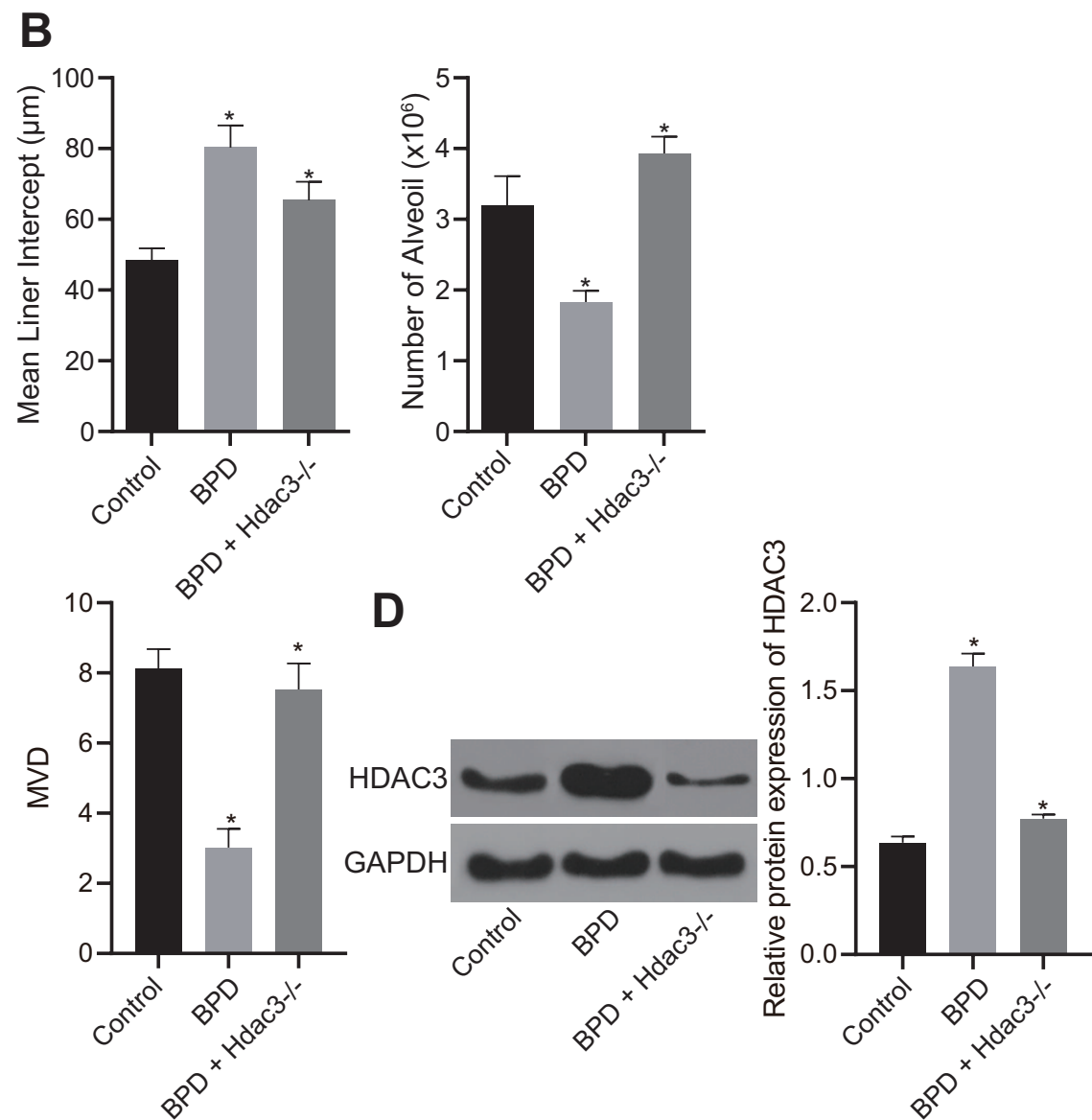
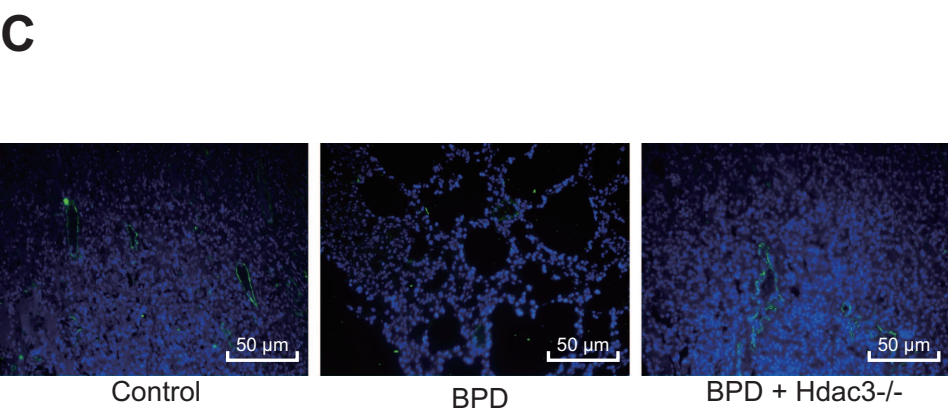
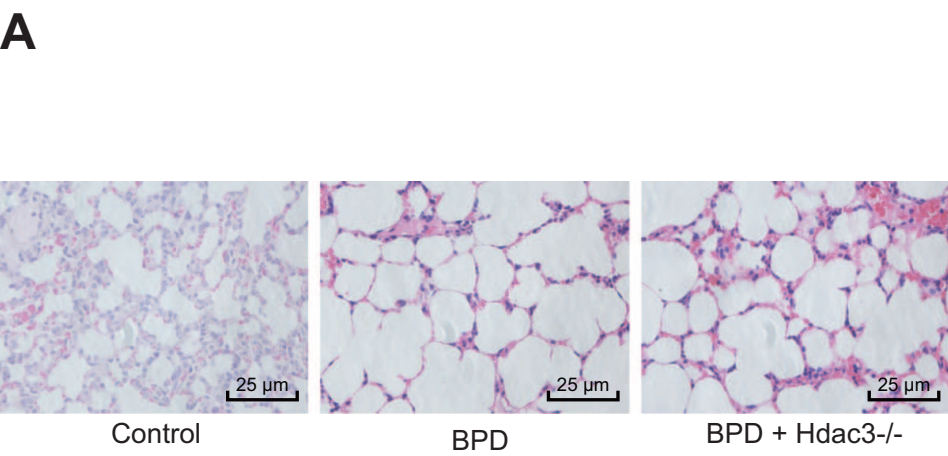
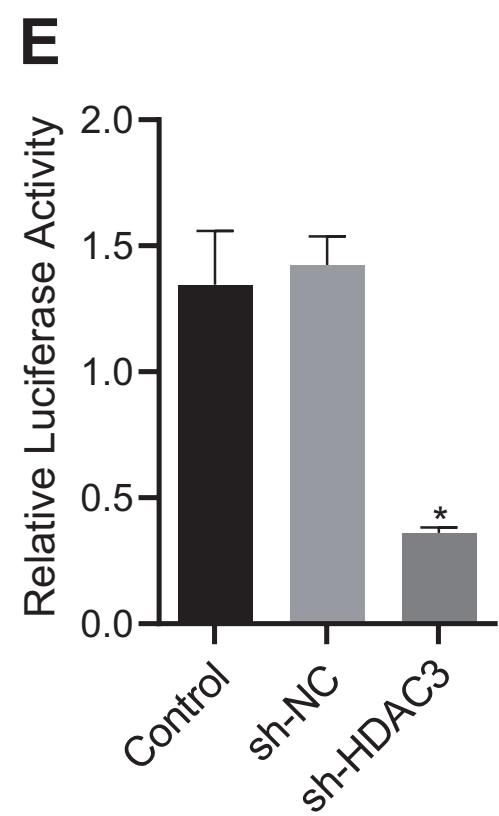
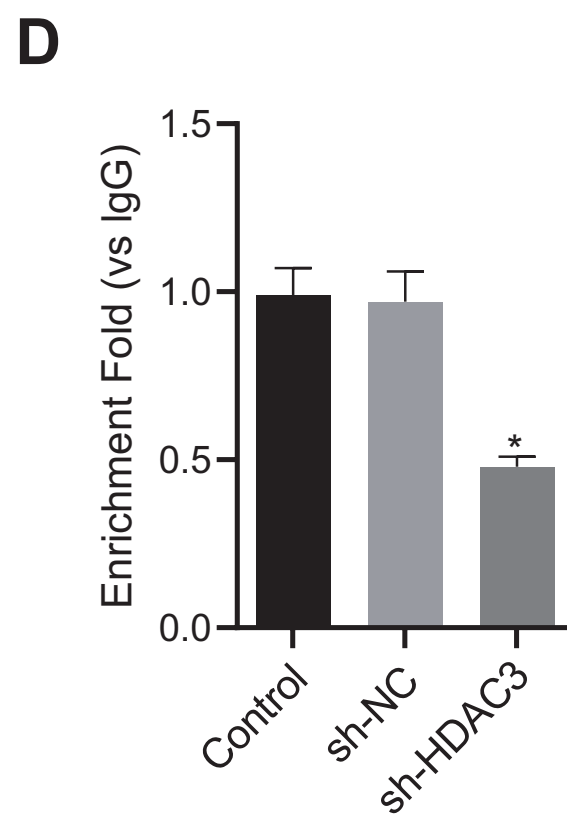
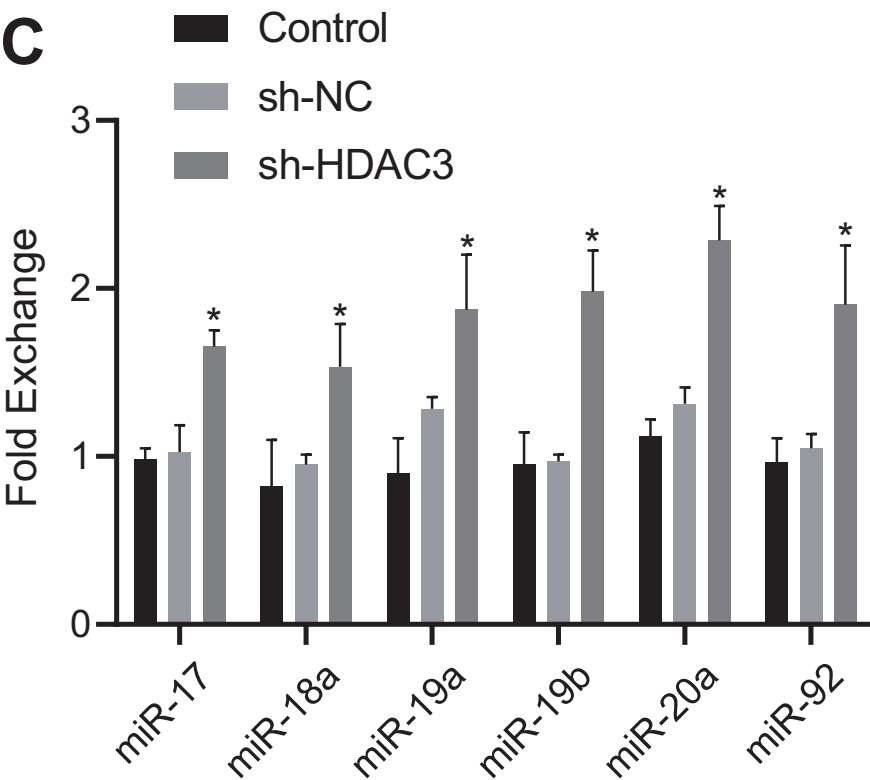
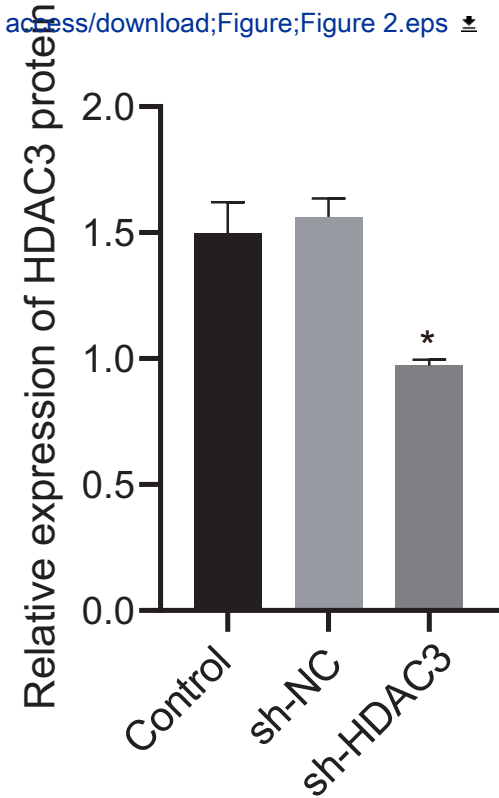
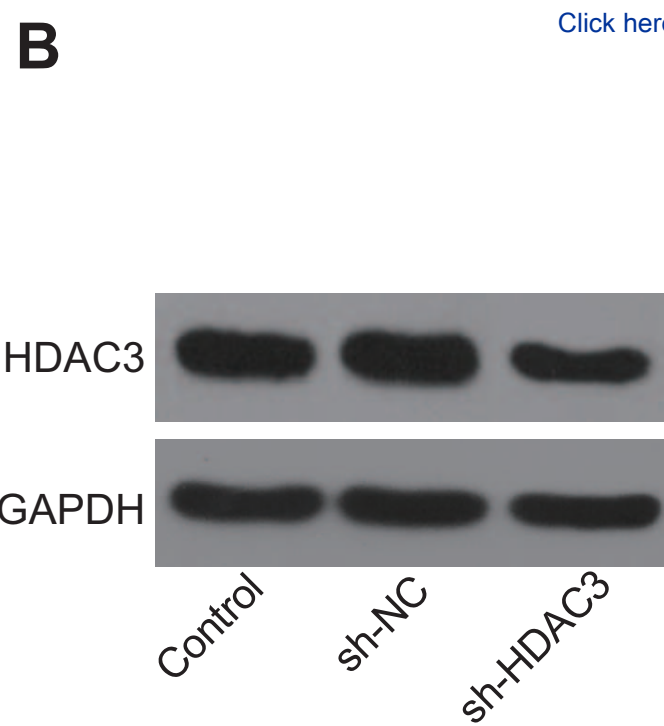
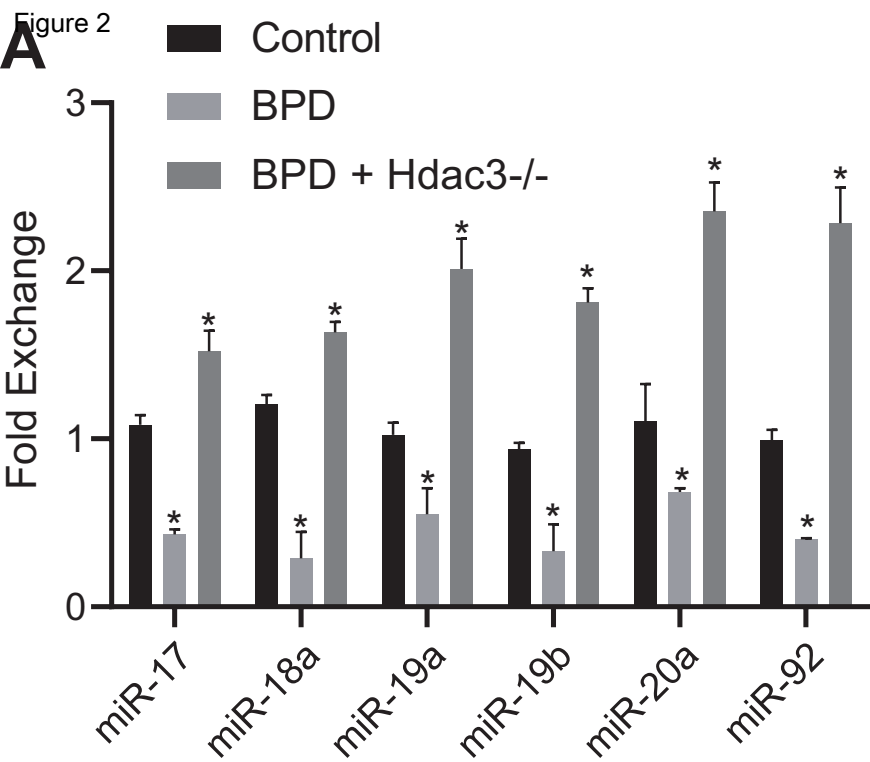
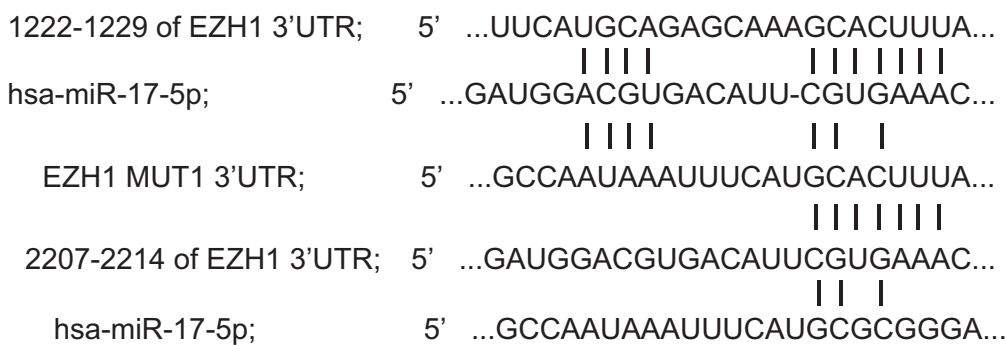
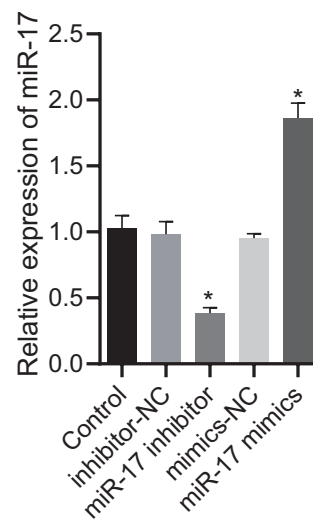
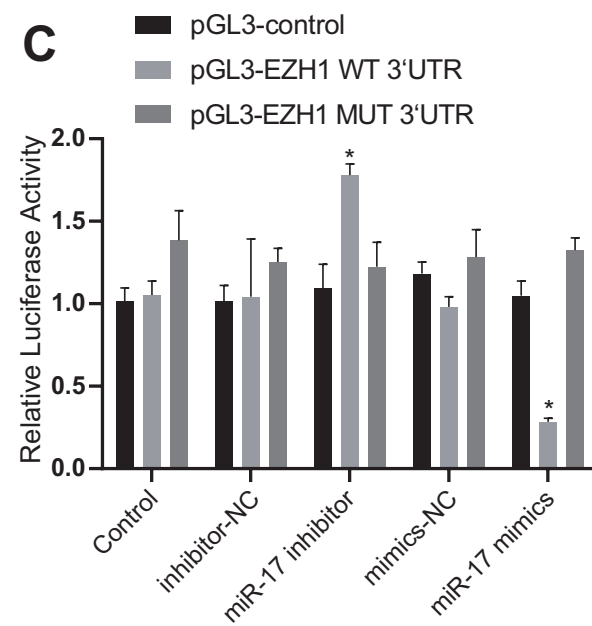
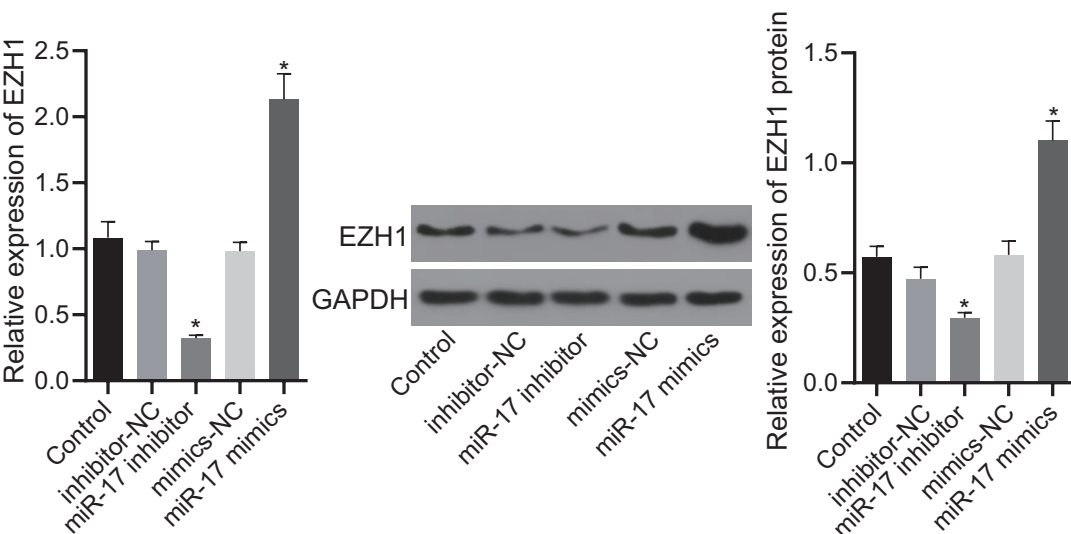
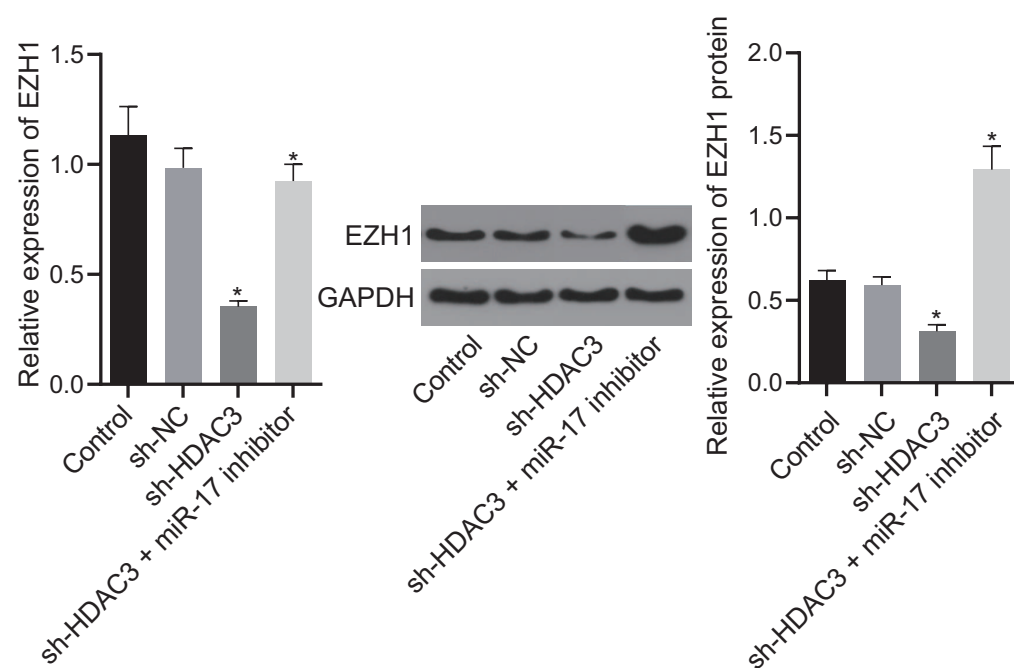


Figure 2



A**B****C****D****E**

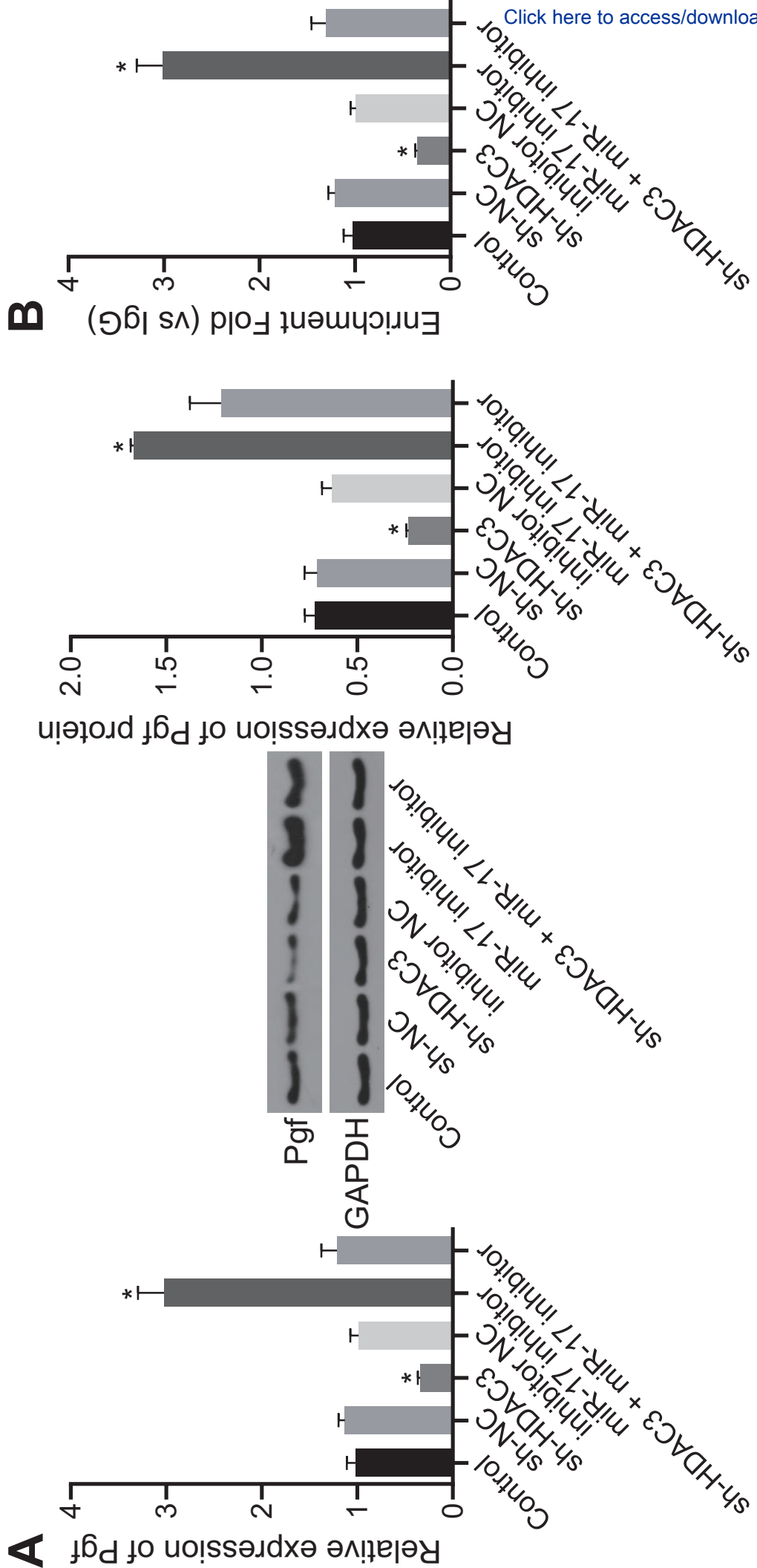
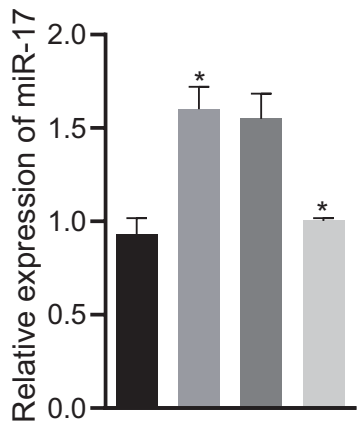


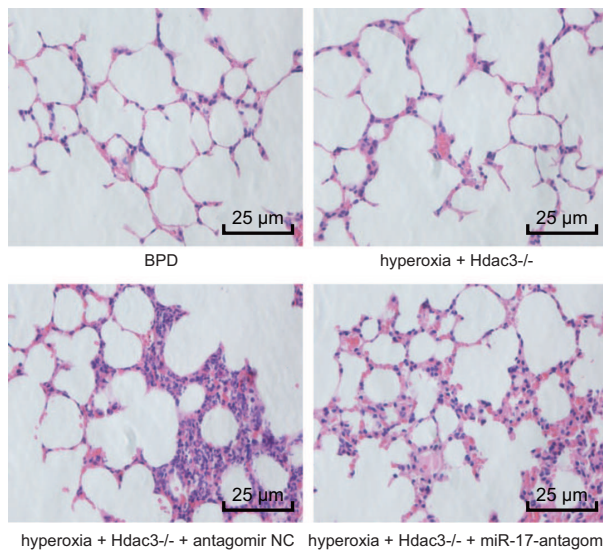
Figure 6

[Click here to access/download;Figure;Figure 6.eps](#)

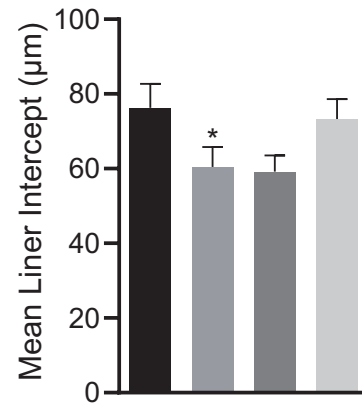
■ BPD
 ■ hyperoxia + Hdac3^{-/-}
 ■ hyperoxia + Hdac3^{-/-} + antagonomir NC
 ■ hyperoxia + Hdac3^{-/-} + miR-17-antagomir



B

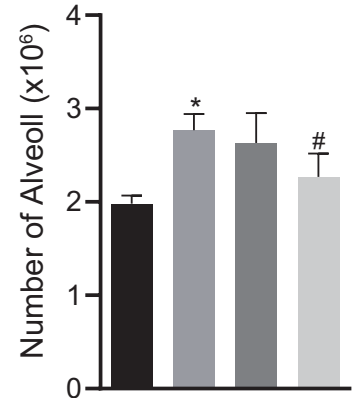


■ BPD
 ■ hyperoxia + Hdac3^{-/-}
 ■ hyperoxia + Hdac3^{-/-} + antagonomir NC
 ■ hyperoxia + Hdac3^{-/-} + miR-17-antagomir

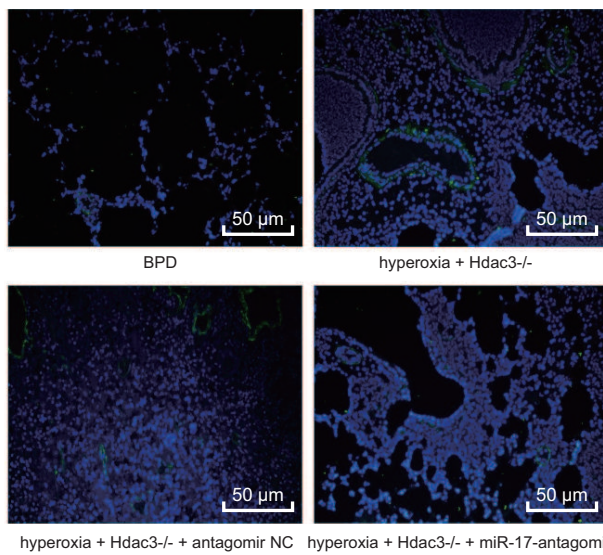


D

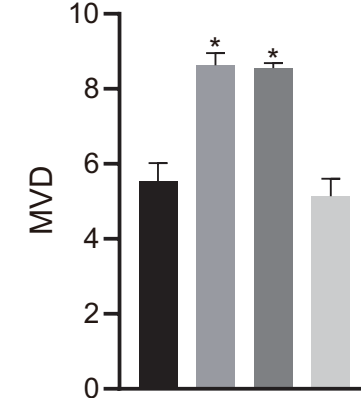
■ BPD
 ■ hyperoxia + Hdac3^{-/-}
 ■ hyperoxia + Hdac3^{-/-} + antagonomir NC
 ■ hyperoxia + Hdac3^{-/-} + miR-17-antagomir



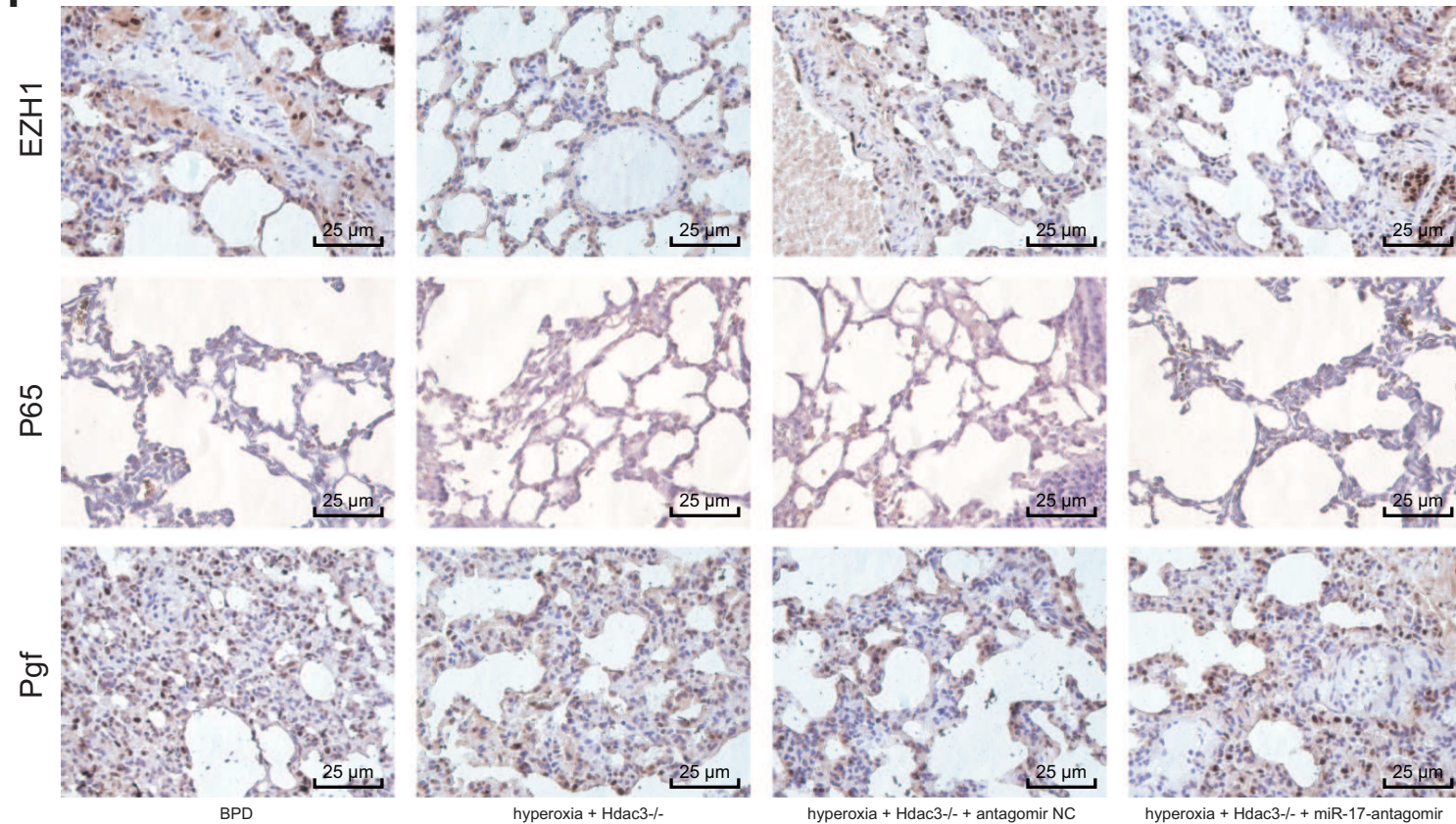
E



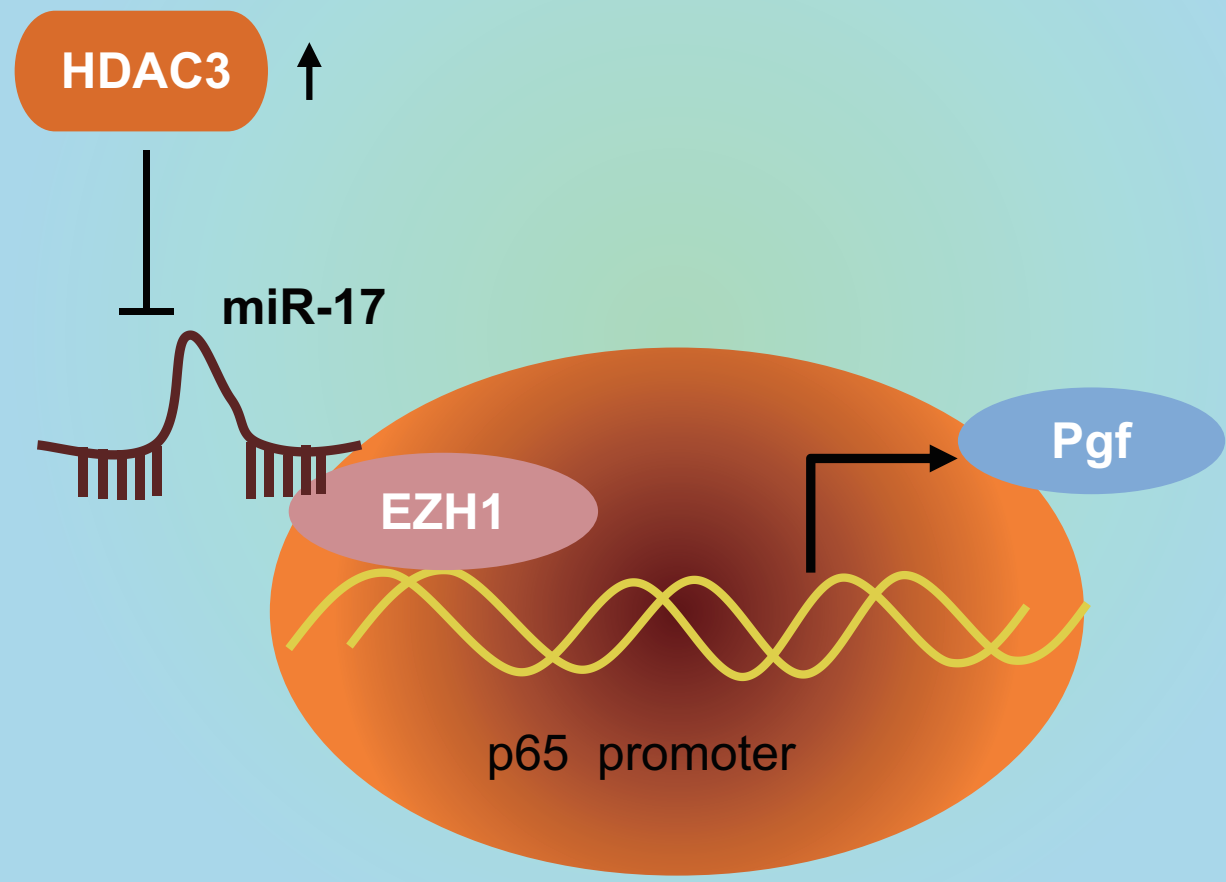
■ BPD
 ■ hyperoxia + Hdac3^{-/-}
 ■ hyperoxia + Hdac3^{-/-} + antagonomir NC
 ■ hyperoxia + Hdac3^{-/-} + miR-17-antagomir



F



Primary mouse lung fibroblasts



bronchopulmonary
dysplasia in neonatal mice